

Acoustomagnetolectric Effect in Graphene Nanoribbon in the Presence of External Electric and Magnetic Fields

Kwadwo A. Dompseh^{a,*}, Samuel Y. Mensah^a, Sulemana S. Abukari^a,
Raymond Edziah^a, Natalia G. Mensah^b, Harrison A. Quaye^c

^a*Department of Physics, College of Agriculture and Natural Sciences, U.C.C, Ghana.*

^b*Department of Mathematics, College of Agriculture and Natural Sciences, U.C.C, Ghana*

^c*Department of Computer Science, College of Agriculture and Natural Sciences, U.C.C, Ghana*

Abstract

Acoustomagnetolectric Effect (AME) in Graphene Nanoribbon (GNR) in the presence of an external electric and magnetic fields was studied using the Boltzmann kinetic equation. On open circuit, the Surface Acoustomagnetolectric field (\vec{E}_{SAME}) in GNR was obtained in the region $ql \gg 1$, for energy dispersion $\varepsilon(p)$ near the Fermi level. The dependence of \vec{E}_{SAME} on the magnetic field strength (η), the sub-band index (p_i), and the width (N) of GNR were analysed numerically. For \vec{E}_{SAME} versus η , a non-linear graph was obtained. From the graph, at low magnetic field strength ($\eta < 0.62$), the obtained graph qualitatively agreed with that experimentally observed in graphite. However, at high magnetic field strength ($\eta > 0.62$), the \vec{E}_{SAME} falls rapidly to a minimum value. We observed that in GNR, the maximum \vec{E}_{SAME} was obtained at magnetic field $H = 3.2Am^{-1}$. The graphs obtained were modulated by varying the sub-band index p_i with an inversion observed

*Corresponding author
Email: kwadwo.dompseh@ucc.edu.gh

when $p_i = 6$. The dependence of \vec{E}_{SAME} on the width N for various p_i was also studied where, \vec{E}_{SAME} decreases for increase in p_i . To enhanced the understanding of \vec{E}_{SAME} on the N and η , a 3D graph was plotted. This study is relevant for investigating the properties of GNR.

Introduction

The study of Acoustomagnetolectric Effect (AME) in Semiconductors and its related materials have generated lot of interest recently . AME in materials such as Superlattices [1, 2, 3], Quantum Wires [4], Carbon Nanotubes [5] deals with appearance of a d.c electric field in the Hall direction when the sample is on open circuit. Studies have shown that the propagation of acoustic waves causes the transfer of energy and momentum to the conducting electrons [3]. When the build up of the acoustic flux exceeds the velocity of sound it causes the formation and propagation of Acoustoelectric field [6, 7]. Other effects such as Acoustoelectric Effect (AE) [1, 2, 8], Acoustothermal Effect [9], and Acoustoconcentration Effect can occur. The AE was predicted by Grinberg and Kramer [10] for bipolar semiconductors and experimentally observed in Bismuth by Yamada [11]. By applying the sound flux (\vec{W}), electric current (\vec{j}), and magnetic fields (\vec{H}) perpendicularly to the sample, it is interesting to note that, with the sample opened in direction perpendicular to the Hall direction, can leads to a non-zero Acoustomagnetolectric Effect AME [12]. Mensah et. al [1] studied these effect in Superlattice in the hypersound regime, Bau et. al. [13] studied the AME of cylindrical quantum wires. Also, AME effect in mono-polar semiconductor for both weak and quantizing field were studied [14]. Experimentally, AME

has been observed in n-InSb [15], and in graphite [16] for $ql \ll 1$. In this paper, AME in graphene nanoribbon is studied. There are differences between graphene and graphite.

Graphene[17] is a single layer of carbon atoms with zero band-gap. Within the low energy range ($\varepsilon < 0.5eV$), carriers in graphenes are massless relativistic particles with effective speed of $V_F \approx 10^6 m.s^{-1}$ (V_F being the Fermi velocity). One of the major limitations of graphene sheet is lack of band gap in its energy spectrum [18]. To overcome this, stripes of Graphene called Graphene Nanoribbons (GNRs) whose characteristics are dominated by the nature of their edges (the armchair (AGNRs) and Zigzag (ZGNRs)) with well-defined width are proposed [18]. By patterning graphene into narrow ribbons creates an energy gap where GNR behaves like semiconductor [19, 20, 21]. However, graphite (bunch of graphene) have planar structures with a semimetallic behaviour having a band overlap of about $4.1MeV$. Its thermal, acoustic and electronic properties are highly anisotropic, which means that phonons travel much easily along the planes than they do through the planes [23]. Graphene therefore have a very high electron mobility thus offers a much better level of electronic conduction. In this paper, the Boltzmann kinetic equation is used to study the SAME in GNR. This is achieved by applying sound flux (\vec{W}) to the GNR sample in the presence of electric field (\vec{E}) and magnetic fields (\vec{H}). With the sample open ($j = 0$), give the E_{SAME} in GNR. This paper is organised as follows: In section 2, the theory of SAME in GNRs is outlined. In section 3, the numerical calculations are presented; and while section 4 deals with the conclusion.

Theory

The configuration for surface Acoustomagnetolectric field in GNR will be considered with the acoustic phonon \vec{W} , the magnetic field \vec{H} and the measured E_{SAME} lying in the same plane. Based on the method developed in [22], the partial current density generated in the sample is solved from the Boltzmann transport equation given as

$$-\left(e\vec{E}\frac{\partial f_{\vec{p}}}{\partial \vec{p}} + \Omega[\vec{p}, \vec{H}], \frac{\partial f_{\vec{p}}}{\partial \vec{p}}\right) = -\frac{f_{\vec{p}} - f_0(\varepsilon_{\vec{p}})}{\tau(\varepsilon_{\vec{p}})} + \frac{\pi\Delta^2\vec{W}}{\rho V_s^3} \{ [f_{\vec{p}+\vec{q}} - f_{\vec{p}}]\delta(\varepsilon_{\vec{p}+\vec{q}} - \varepsilon_{\vec{p}} - \hbar\omega_{\vec{q}}) + [f_{\vec{p}-\vec{q}} - f_{\vec{p}}]\delta(\varepsilon_{\vec{p}-\vec{q}} - \varepsilon_{\vec{p}} + \hbar\omega_{\vec{q}}) \} \quad (1)$$

where $ql \gg 1$ is utilised. Here, $f_0(\varepsilon(\vec{p}))$ is the equilibrium distribution function, \vec{E} is the constant electric field, $\omega_{\vec{q}}$ is the frequency of the acoustic wave, \vec{W} is the density of the acoustic flux, and \vec{p} the characteristic quasi-momentum of the electron. ρ is the density of the sample, Δ is the constant of deformation potential, e the electronic charge, and V_s is the speed of sound. The relaxation time on energy is $\tau(\varepsilon_{\vec{p}})$ and the cyclotron frequency, $\Omega = \mu H/\hbar c$ (H is the magnetic field, μ is the electron mobility and c is the speed of light in vacuum). The energy dispersion relation $\varepsilon(\vec{p})$ for GNRs band near the Fermi point is expressed as [18, 24]

$$\varepsilon(\vec{p}) = \frac{E_g}{2} \sqrt{\left[1 + \frac{\vec{p}^2}{\hbar^2\beta^2}\right]} \quad (2)$$

where the energy gap $E_g = 3ta_{c-c}\beta$ with β being the quantized wave vector given as $\beta = \frac{2\pi}{a\sqrt{3}}[\frac{p_i}{N+1} - \frac{2}{3}]$, where p_i is the sub-band index and N is the width of the GNR. $t = 2.7\text{eV}$ is the nearest neighbour Carbon-Carbon C-C tight binding overlap energy and $a_{c-c} = 1.42\text{\AA}$ is the (C-C) bond length.

Multiplying the Eqn.(1) by $\vec{p}\delta(\varepsilon - \varepsilon_{\vec{p}})$ and summing over \vec{p} gives the kinetic equation as

$$\frac{\vec{R}(\varepsilon)}{\tau(\varepsilon)} + \Omega \left[\vec{h}, \vec{R}(\varepsilon) \right] = \vec{\Lambda}(\varepsilon) + \vec{S}(\varepsilon) \quad (3)$$

where $\vec{R}(\varepsilon)$ is the partial current density given as

$$\vec{R}(\varepsilon) \equiv e \sum_{\vec{p}} \vec{p} f_{\vec{p}} \delta(\varepsilon - \varepsilon_{\vec{p}}) \quad (4)$$

with $\vec{\Lambda}(\varepsilon)$ and $\vec{S}(\varepsilon)$ given as

$$\vec{\Lambda}(\varepsilon) = -e \sum_{\vec{p}} \left(\vec{E}, \frac{\partial f_{\vec{p}}}{\partial \vec{p}} \right) \vec{p} \delta(\varepsilon - \varepsilon_{\vec{p}}) \quad (5)$$

$$\vec{S}(\varepsilon) = \frac{\pi \Delta^2 \vec{W}}{\rho V_s^3} \sum_{\vec{p}} \vec{p} \delta(\varepsilon - \varepsilon_{\vec{p}}) \{ [f_{\vec{p}+\vec{q}} - f_{\vec{p}}] \delta(\varepsilon_{\vec{p}+\vec{q}} - \varepsilon_{\vec{p}} - \hbar \omega_{\vec{q}}) + [f_{\vec{p}-\vec{q}} - f_{\vec{p}}] \delta(\varepsilon_{\vec{p}-\vec{q}} - \varepsilon_{\vec{p}} + \hbar \omega_{\vec{q}}) \} \quad (6)$$

Considering $f_{\vec{p}} \rightarrow f_0(\varepsilon_{\vec{p}})$ with $\vec{p} \rightarrow -\vec{p}$, $f_{\vec{p}} \equiv f_0(\varepsilon_{\vec{p}}) = f_0(\varepsilon_{-\vec{p}})$, Eqn.(5) and Eqn.(6) can be respectively expressed to

$$\vec{\Lambda}(\varepsilon) = \vec{E} \left(\frac{2\hbar^2 \beta^2}{\hbar \vec{q}} \alpha - \frac{\hbar \vec{q}}{2} \right) \frac{\partial f_0}{\partial \varepsilon} \frac{\Theta(1 - \alpha^2)}{\sqrt{1 - \alpha^2}} \quad (7)$$

$$\vec{S}(\varepsilon) = \frac{2\pi \vec{W}}{\rho V_s \alpha} \Gamma_0 \left(\frac{2\hbar^2 \beta^2}{\hbar \vec{q}} \alpha - \frac{\hbar \vec{q}}{2} \right) \frac{\Theta(1 - \alpha^2)}{\sqrt{1 - \alpha^2}} \frac{1}{f_0(\varepsilon)} \frac{\partial f_0}{\partial \varepsilon} \quad (8)$$

with $\alpha = \hbar \omega_{\vec{q}}/E_g$, $\Gamma_0 = (E_g^2 \Delta^2 \alpha^2 / 2V_s^2) f_0(\varepsilon)$ and Θ is the Heaviside step function given as

$$\Theta(1 - \alpha^2) = \begin{cases} 1 & \text{if } (1 - \alpha^2) > 0 \\ 0 & \text{if } (1 - \alpha^2) < 0 \end{cases}$$

Substituting Eqn.(7) and Eqn.(8) into Eqn.(3) and solving for $\vec{R}(\varepsilon)$ gives

$$\begin{aligned} \vec{R}(\varepsilon) = & \left\{ \frac{2\pi}{\rho V_s \alpha} \Gamma_0 \left(\frac{2\hbar^2 \beta^2}{\hbar \vec{q}} \alpha - \frac{\hbar \vec{q}}{2} \right) \frac{\Theta(1-\alpha^2)}{\sqrt{1-\alpha^2}} \frac{1}{f_0(\varepsilon)} \frac{\partial f_0}{\partial \varepsilon} \times \right. \\ & \left. \{ \vec{W} \tau(\varepsilon) + \Omega [\vec{h}, \vec{W}] \tau(\varepsilon)^2 + \Omega^2 \vec{h}(\vec{h}, \vec{W}) \tau(\varepsilon)^3 \} + \left(\frac{2\hbar^2 \beta^2}{\hbar \vec{q}} \alpha - \frac{\hbar \vec{q}}{2} \right) \frac{\partial f_0}{\partial \varepsilon} \frac{\Theta(1-\alpha^2)}{\sqrt{1-\alpha^2}} \times \right. \\ & \left. \{ \vec{E} \tau(\varepsilon) + \Omega [\vec{h}, \vec{E}] \tau(\varepsilon)^2 + \Omega^2 \tau(\varepsilon)^3 \vec{h}(\vec{h}, \vec{E}) \} \right\} \{1 + \Omega^2 \tau(\varepsilon)^2\}^{-1} \quad (9) \end{aligned}$$

The current density [6] is given as

$$\vec{j} = - \int_0^\infty \vec{R}(\varepsilon) d\varepsilon \quad (10)$$

With $\Delta = \left(\frac{2\hbar^2 \beta^2}{\hbar \vec{q}} \alpha - \frac{\hbar \vec{q}}{2} \right)$, substituting Eqn.(9) into Eqn.(10) yields

$$\begin{aligned} \vec{j} = & \frac{\Delta \Gamma_0}{\rho V_s \alpha} \frac{\Theta(1-\alpha^2)}{\sqrt{1-\alpha^2}} \left\{ \left\langle \left\langle \frac{\tau(\varepsilon)}{1 + \Omega^2 \tau(\varepsilon)^2} \right\rangle \right\rangle \vec{W} + \Omega \left\langle \left\langle \frac{\tau(\varepsilon)^2}{1 + \Omega^2 \tau(\varepsilon)^2} \right\rangle \right\rangle [\vec{h}, \vec{W}] + \right. \\ & \Omega^2 \left\langle \left\langle \frac{\tau(\varepsilon)}{1 + \Omega^2 \tau(\varepsilon)^2} \right\rangle \right\rangle \vec{h}(\vec{h}, \vec{W}) \left. \right\} + \Delta \frac{\Theta(1-\alpha^2)}{\sqrt{1-\alpha^2}} \left\{ \left\langle \frac{\tau(\varepsilon)}{1 + \Omega^2 \tau(\varepsilon)^2} \right\rangle \vec{E} + \Omega \left\langle \frac{\tau(\varepsilon)^2}{1 + \Omega^2 \tau(\varepsilon)^2} \right\rangle [\vec{h}, \vec{E}] + \right. \\ & \left. \Omega^2 \left\langle \frac{\tau(\varepsilon)^3}{1 + \Omega^2 \tau(\varepsilon)^2} \right\rangle \vec{h}(\vec{h}, \vec{E}) \right\} \quad (11) \end{aligned}$$

The Eqn.(11) can further be simplified with the following substitution $g = 1/1 + \Omega^2 \tau(\varepsilon)^2$, $\gamma_k \equiv \langle g \tau(\varepsilon)^k \rangle$, and $\eta \equiv \langle \langle g \tau(\varepsilon)^k \rangle \rangle$ where $k = 1, 2, 3$. This yields

$$\begin{aligned} \vec{j} = & \frac{\Delta \Gamma_0}{\rho V_s \alpha} \frac{\Theta(1-\alpha^2)}{\sqrt{1-\alpha^2}} \left\{ \eta_1 \vec{W} + \Omega \eta_2 [\vec{h}, \vec{W}] + \Omega^2 \eta_3 \vec{h}(\vec{h}, \vec{W}) \right\} + \\ & \Delta \frac{\Theta(1-\alpha^2)}{\sqrt{1-\alpha^2}} \left\{ \gamma_1 \vec{E} + \gamma_2 \Omega [\vec{h}, \vec{E}] + \Omega^2 \gamma_3 \vec{h}(\vec{h}, \vec{E}) \right\} \quad (12) \end{aligned}$$

With the sample opened ($\vec{j} = 0$), and ignoring higher powers of Ω gives

$$\gamma_1 \vec{E}_x - \gamma_2 \Omega \vec{E}_y = -\gamma_1 \vec{E}_\alpha \quad (13)$$

$$\gamma_2 \Omega \vec{E}_x + \gamma_2 \Omega \vec{E}_y = -\gamma_2 \Omega \vec{E}_\alpha \quad (14)$$

where $E_\alpha = \frac{\Gamma_0}{\rho S_\alpha}$. Making the \vec{E}_y the subject of the equation yields

$$\vec{E}_y = \vec{E}_\alpha \Omega \left\{ \frac{\eta_1 \gamma_2 - \eta_2 \gamma_1}{\gamma_1^2 + \gamma_2^2 \Omega^2} \right\} \quad (15)$$

substituting the expressions for $\eta_1, \eta_2, \gamma_1, \gamma_2$ into Eqn.(15), with $\vec{E}_y = \vec{E}_{SAME}$ gives

$$\vec{E}_{SAME} = \vec{E}_\alpha \Omega \left\{ \frac{\langle \frac{\tau(\varepsilon)^2}{1+\Omega^2 \tau(\varepsilon)^2} \rangle \langle \frac{\tau(\varepsilon)}{1+\Omega^2 \tau(\varepsilon)^2} \rangle - \langle \frac{\tau(\varepsilon)^2}{1+\Omega^2 \tau(\varepsilon)^2} \rangle \langle \frac{\tau(\varepsilon)}{1+\Omega^2 \tau(\varepsilon)^2} \rangle}{\langle \frac{\tau(\varepsilon)}{1+\Omega^2 \tau(\varepsilon)^2} \rangle^2 + \langle \frac{\tau(\varepsilon)^2}{1+\Omega^2 \tau(\varepsilon)^2} \rangle^2 \Omega^2} \right\} \quad (16)$$

In Eqn(16), the following averages were used

$$\begin{aligned} \langle \dots \rangle &= - \int_0^\infty (\dots) \frac{\partial f_0}{\partial \varepsilon} d\varepsilon \\ \langle \langle \dots \rangle \rangle &= - \frac{2\pi}{f_0(\varepsilon)} \int_0^\infty (\dots) \frac{\partial f_0}{\partial \varepsilon} d\varepsilon \end{aligned}$$

Where $f_0 = [1 - \exp(-\frac{1}{kT}(\varepsilon - \varepsilon_F))]^{-1}$ is the Fermi-Dirac distribution function.

Numerical analysis and Discussions

In solving for Eqn.(16), the following were assumed: At low temperature $kT \ll 1$, and $\frac{\partial f_0}{\partial \varepsilon} = \frac{-1}{k_\beta T} \exp(-\frac{\varepsilon - \mu}{k_\beta T})$. The equation for \vec{E}_{SAME} simplifies to

$$\begin{aligned} \vec{E}_{SAME} = \frac{E_g \vec{W} \hbar \omega_q \eta}{2\rho V_s^3} \{ F_{(-1/2, \eta^2)} F_{(-3/2, \eta^2)} - F_{(0, \eta^2)} F_{(-2, \eta^2)} \} \times \\ \left\{ \frac{3\sqrt{\pi}}{4} F_{(-1/2, \eta^2)}^2 + \frac{9\pi}{16} \eta^2 F_{(0, \eta^2)}^2 \right\}^{-2} \end{aligned} \quad (17)$$

with $F_{m,n} = \int_0^\infty \frac{x^m}{1+\Omega^2 \tau(\varepsilon)^2 x^n} \frac{\partial f_0(\varepsilon)}{\partial x} dx$. From Eqn.(17), the \vec{E}_{SAME} is a function of the following parameters: magnetic field strength ($\eta = \Omega \tau$); α ; and the energy gap $E_g = 3ta_{c-c}\beta$. The E_g depends on the quantized wave vector β . The parameters used in the numerical calculations are $\tau = 10^{-12}s$, $\omega_q =$

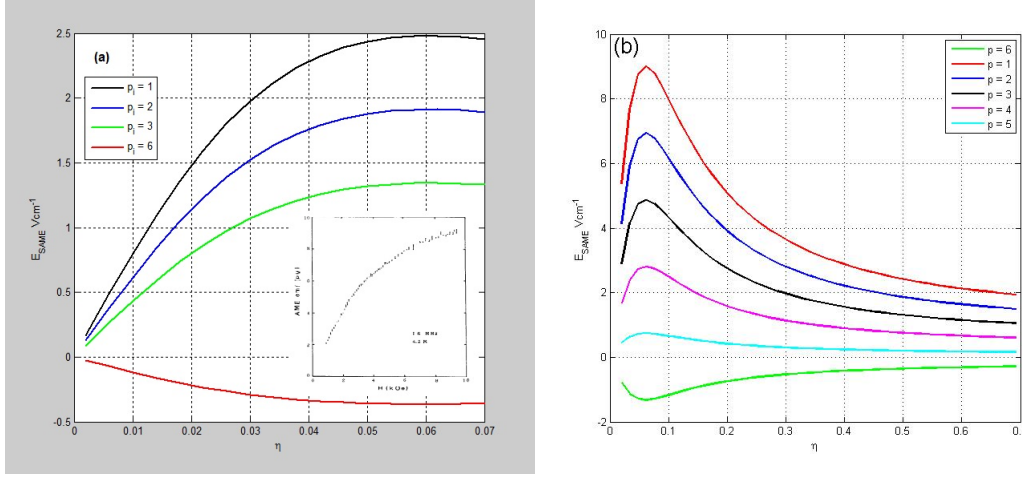


Figure 1: Dependence of \vec{E}_{SAME} versus the magnetic field strength η for (a) $N = 7$ -GNR at different sub-bands. The insert shows the experimental observation of \vec{E}_{AME} in graphite [16]. (b) an extended graph of \vec{E}_{SAME} against η

10^{10}s^{-1} , $s = 5 * 10^3 \text{ms}^{-1}$, $q = 2.23 * 10^6 \text{cm}$. In analysing the Eqn.(17), the condition $((1 - \alpha^2) > 0)$ was considered. Figure 1a, shows the dependence of \vec{E}_{SAME} against the magnetic field strength η at various sub-bands for $\eta \ll 1$. Generally, \vec{E}_{SAME} increased to a maximum value for three different values of p_i . The results obtained (see Figure 1a) qualitatively agreed with an experimental graph measured in graphite. Figure 1b is the general case when there is no limitation on η . It can be seen that, \vec{E}_{SAME} decreased rapidly after the maximum point to a minimum value. For $p_i = 6$, there is an inversion of the graph. Figure 2, shows the dependence of \vec{E}_{SAME} against the width N with different sub-band indices (p_i). For further illucidation of the graphs obtained, a 3D graph of \vec{E}_{SAME} versus η at $p_i = 1$ and width at $p_i = 6$ are presented (see Figure 3 a and b) where Figure 3b shows an inversion of Figure 3a.

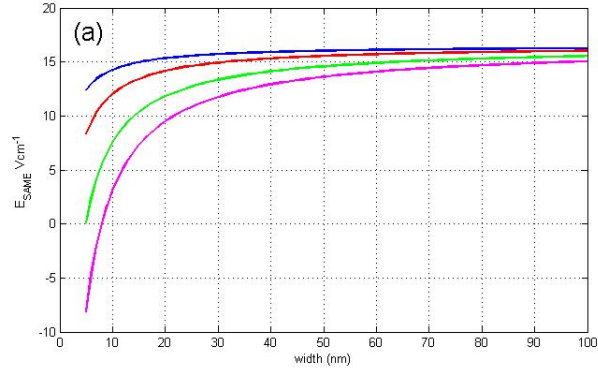


Figure 2: (a) The \vec{E}_{SAME} versus width for $p = 1, 3, 5$.

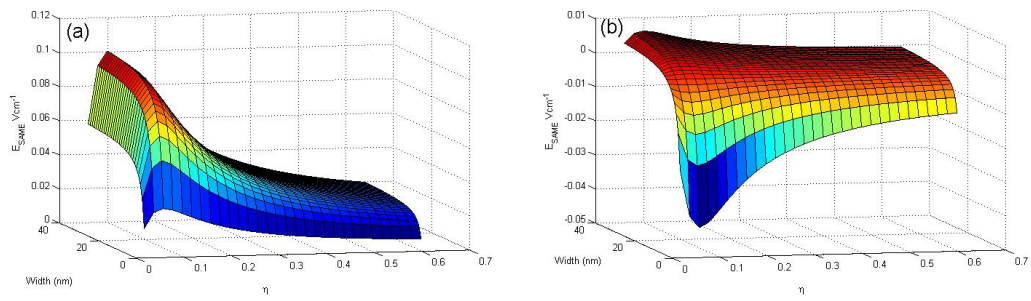


Figure 3: A 3D graph of \vec{E}_{SAME} on width of GNR and η (a) $p = 1$ and (b) $p = 6$.

Conclusions

The Acoustomagnetolectric field E_{SAME} in Graphene Nanoribbon (GNR) was studied. The dependence of E_{SAME} on the magnetic field strength η and the width N were numerically studied. The E_{SAME} obtained for low magnetic field strength in GNR qualitatively agreed with experimentally observed graph in graphite but for strong magnetic fields, the E_{SAME} rapidly falls to a minimum. The graph is modulated by varying the sub-band index p_i with an inversion occurring at $p_i = 6$. or the width N of GNR. At the maximum point, a magnetic field of $H = 3.2Am^{-1}$ was calculated which is far lower than that measured in graphite. The E_{SAME} also varies when plotted against the Width of GNR at various sub-band indices p_i .

Bibliography

- [1] Mensah, S. Y. and F. K. A. Allotey, *AE effect in semiconductor SL*, J. Phys: Condens.Matter., Vol. 6, 6783, (1994).
- [2] Mensah, S. Y. and F. K. A. Allotey, *Nonlinear AE effect in semiconductor SL*, J. Phys.: Condens. Matter. Vol. 12, 5225, (2000).
- [3] Mensah, S. Y., Allotey, F. K. A., and Adjepong, S. K., *Acoustomagneto-electric effect in a superlattice*, J. Phys. Condens. Matter 8 1235-1239, (1996).
- [4] Nghia, N. V., Bau, N. Q., Vuong, D. Q. *Calculation of the Acoustomagnetolectric Field in Rectangular Quantum Wire with an Infinite Potential in the Presence of an External Magnetic Field*, PIERS Proceedings, Kuala Lumpur, MALAYSIA 772 - 777, (2012).

- [5] Reulet, B., Kasumov, A. Yu., Kociak, M., Deblock, R., Khodos I. I., Gorbatov, Yu. B., Volkov, V. T., Journet, C., Bouchiat, H., *Acousto-electric effect in carbon nanotubes*, Phys. Review Letters, Vol. 85, No. 13, (2000).
- [6] Mensah, N. G. *Acoustomagnetolectric effect in degenerate Semiconductor with non-parabolic energy dispersion law*, arXiv.cond-mat.1002.3351, (2006)
- [7] Zhang, S. H., Xu, W., *Absorption of Surface acoustic waves by graphene*, AIP Advances, 1, 022146 (2011).
- [8] Maaouf, F. A., Galperin Y., Phys.: Rev. B 56 (1997) 4028
- [9] Mensah, S. Y., and Kangah, G. K., J. Phy.: Condens. Matter. 3, (1991) 4105.
- [10] Grinberg, A. A., and Kramer, N. I., Sov. Phys., Doklady (1965) Vol. 9., No. 7552.
- [11] Yamada, T., J. Phys. Soc. Japan (1965) 20 1424.
- [12] Shmelev, G. M., Nguyen Quoc Anh, Tsurkan, G. I., and Mensah S. Y., *currentless Amplification of hypersound in a planar configuration by inelastic scattering of electrons*, phys. stat. sol. (b) 121, 209, (1984).
- [13] Bau, N. Q., N. V. Nhan, and N. V. Nghia, *The dependence of the acoustomagnetolectric current on the parameters of a cylindrical quantum wire with an infinite potential in the presence of an external magnetic field*, PIERS Proceedings, 14521456, Suzhou, China, Sep. 1216, 2011.

- [14] Shmelev, G. M., G. I. Tsurkan, and N. Q. Anh, *Photostimulated planar acoustomagnetolectric effect in semiconductors*, Phys. Stat. Sol., Vol. 121, No. 1, 97102, 1984.
- [15] Kogami, M., and Tanaka, SH., J. Phys. Soc. Japan 30, 775 (1971).
- [16] Ohashi, F., Kimura, K., and Sugihara, K., Physica 105B, 103 (1981).
- [17] Novoselov, K. S., Geim, A. K., Morozov, S. V., Jiang, D., Zhang, Y., Dubonos, S. V., Grigorieva, I. V., and Firsov, A. A., Science 306, 666, (2004).
- [18] Huaixiu Z., Zhengfei W., Tao L., Qinwei S., and Jie C., *Analytical study of electronic structure in Armchair Graphene Nanoribbons*, arXiv.cond-mat.0612378v2, (2006).
- [19] Son Y. W., Cohen M. L., and Louie S. G. *Energy Gaps in Graphene Nanoribbons*. Physical Review Letters 97 (21), (2006).
- [20] Mahdi M., Hamed N., Mahdi P., Morteza F., and Hans K., *Analytical models of approximate for wave functions and energy dispersion in zigzag graphene nanoribbons*, J. Applied Physics 111, 074318, (2012).
- [21] Yu-Ming Lin, Vasili Perebeinos, Zhihong Chen, and Phaedon Avouris, *Electrical observation of sub band formation in graphene nanoribbon*, Phy. Review B 78, 161409 (2008).
- [22] Dompreeh, K. A., Mensah, S. Y., Abukari, S. S., Sam, F., and Mensah, N. G., *Amplification of acoustic waves in Armchair graphene nanoribbon*

in the presence of external electric and magnetic field. arXiv:cond-mat. 1101436, (2014).

- [23] Hone, J., Batlogg, B., Benes, Z., Johnson, A. T., Fischer, J. E. , Science 289, 1730 (2000) 279, 280
- [24] Ahmadi, M. T., Johari, Z., Amin, A. N., Fallapour, A. H., Ismail, R., *Graphene Nanoribbon Conductance Model in Parabolic Band Structure*, J. of Nanomaterials, 753738, (2010).